Submitted to

International Europhysics Conference on High Energy Physics, EPS05, July 21-27, 2003, Lisboa
(Abstract **629** Parallel Session **Hard QCD**)

www-h1.desy.de/h1/www/publications/conf/conf_list.html

Inclusive Jet Production in Deep Inelastic Scattering at High Q^2 at HERA

H1 Collaboration

Abstract

The inclusive jet production in deep inelastic positron-proton scattering at HERA is studied. The data sample corresponds to an integrated luminosity of $\mathcal{L}_{int} \sim 61.25$ pb^{-1} and was taken in the years 1999-2000 with the H1 detector at a centre-of-mass energy $\sqrt{s} = 319$ GeV. The measured jet cross section is compared to perturbative QCD calculations using the NLO program NLOJET++, and the strong coupling α_s is extracted.

1 Introduction

Jet production at HERA in neutral current (NC) deep inelastic scattering (DIS) provides an important testing ground for QCD. Jet data are precise at high transverse energy, where experimental systematic uncertainties and non-perturbative effects are small. Measurements of jet cross sections allow to test the understanding of calculational techniques in perturbative QCD, to extract the strong coupling α_s and to constrain the proton and photon parton distribution functions (PDFs). Here, we report on a measurement of the inclusive jet cross section in NC DIS at high momentum transfers Q^2 and a determination of the strong coupling constant $\alpha_s(M_Z)$.

1.1 Deep Inelastic Scattering

The kinematics of DIS are defined via the four momenta of the incoming (k) and outgoing electron (k'), incoming proton (p) and exchanged boson ($q = k - k'$):

$$\begin{array}{ll} s = (k+p)^2 \simeq 4E_e E_p, & Q^2 = -q^2 = -(k-k')^2, \\ x = Q^2/(2pq), & y = Q^2/sx, \end{array}$$

where s is the centre-of-mass energy, Q^2 the negative four momentum transfer squared, x the Bjørken scaling variable, and y the inelasticity. There are several methods to reconstruct the kinematic variables in NC DIS events, since there is redundant information on the reconstructed level from both, the lepton and the hadronic final state. Commonly used methods are referred to as the electron method, the hadron method, the Σ method, the electron-Σ method and the double angle method. Similarly to a published H1 analysis [1], the present study uses the electron-Σ method to calculate the kinematic variables.

1.2 Jet Production in Deep Inelastic Scattering

The factorisation property for the calculation of jet production in DIS is only given in selected frames [2]. In the present analysis the Breit frame of reference is used. By selecting high transverse energy (E_t) jets in this frame, contributions from the Born level and jets induced by the beam remnant are suppressed (Fig. 1). The lowest order contributions to jet production in the Breit frame are of order $\mathcal{O}(\alpha_s)$ and hence directly sensitive to QCD radiation. The scope of the present analysis is on the following differential inclusive jet cross sections: $\mathrm{d}^2\sigma_{jet}/\mathrm{d}Q^2\mathrm{d}E_t$, $\mathrm{d}\sigma_{\mathrm{jet}}/\mathrm{d}Q^2$ and $\mathrm{d}\sigma_{\mathrm{jet}}/\mathrm{d}E_t$.

2 Event and jet selection

The inclusive jet analysis is based on data taken with the H1 detector [3] during the years 1999 to 2000, corresponding to an integrated luminosity of 61.25 pb^{-1} at a centre-of-mass energy $\sqrt{s} = 319$ GeV. High Q^2 DIS events are identified by the detection of a scattered electron in LAr calorimeter. The main selection cuts are briefly listed below.

- $150 < Q^2 < 5000$ GeV^2 and $0.2 < y < 0.6$, where Q^2 and y are obtained using the electron-Σ method.
- Scattered electron energy $E_e > 11\,\mathrm{GeV}$ and $\theta_\mathrm{e} < 153^o$ [1].
- $45 < \sum(E - p_z) < 65\,\mathrm{GeV}$, where the sum is over all hadronic final state particles and the electron. Further non-ep background is rejected by recognition of characteristic topologies.
- Jets
  - Jets are defined by the k_t jet finder in the Breit frame.
  - Jet selection: $E_\mathrm{t} > 7$ GeV and $-1.0 < \eta^\mathrm{Lab} < 2.5$.

3 Correction procedure

In order to extract the cross sections, the experimental data are corrected for limited detector acceptance and resolution as well as for QED radiative effects. The phase space of the cross sections is defined by:

$$150 < Q^2 < 5000\,\mathrm{GeV}^2, \quad 0.2 < y < 0.6, \quad E_\mathrm{t} > 7\text{ GeV}, \quad -1.0 < \eta^\mathrm{Lab} < 2.5.$$

The correction factors are determined by the Monte Carlo event generators DjangoH 1.2 (using the Color Dipole Model with Ariadne) and Rapgap 2.8 (LO matrix elements plus parton showers). Both, Rapgap and Django describe the shape of the distributions from the inclusive jet sample (Figs 2 - 3).

The bin-by-bin correction method is employed to obtain the correction factors. Two event samples are generated for each generator: the first sample, which includes QED radiation, is subject to a detector simulation. The second sample is generated with identical setup but without QED radiation and without detector simulation. The correction factor in a bin is obtained as a ratio of the number of events in this bin of the second sample to that of in the first sample.

The arithmetic mean of Rapgap and Django are used as correction factors, while half of the difference is assigned for the model uncertainty. The correction factors differ by less than 20% from unity for most of the bins, and the model dependence in most of the bins is below 10%.

[1] The polar angle θ is defined w.r.t the z-axis. In the H1 coordinate systems the z-axis points in the direction of the proton beam.

4 Experimental Uncertainties

Various sources contribute to the systematic uncertainty of the measured inclusive jet cross section, such as the luminosity measurement, the hadronic and electromagnetic energy scales of the calorimeters, and the momentum scale and angle of the tracks. These individual contributions are determined from the data and are added in quadrature. Another important uncertainty is due to the model dependence in the determination of correction factors. With respect to correlations, the uncertainties are divided into three classes:

- Correlated sources: luminosity measurement uncertainty and positron polar angle.
- Uncorrelated sources: statistical uncertainty and positron azimuthal angle.
- Sources, equally shared between correlated and uncorrelated ones: positron energy scale, LAr energy scale, track momentum and model dependence.

The major experimental uncertainty is due to the the model dependence and the LAr energy scale.

5 NLO QCD calculation

The fixed order calculation program NLOJET++ [5] is used to perform the QCD analysis.

NLOJET++ calculates jet cross sections at parton level, hence one needs to apply hadronisation correction factors to the NLOJET++ prediction in order to compare it with the measured data points. Here, the hadronisation correction is calculated as $(1 + \delta_{\mathrm{had}}) = \sigma_{\mathrm{had}}/\sigma_{\mathrm{part}}$ for Monte Carlo data without QED radiation. Again, results from Rapgap and Django are averaged, and half of the difference is used as uncertainty. The hadronisation corrections for the inclusive jet sample are typically 1.0 to 1.1. Rather large hadronisation corrections (up to 1.4) are observed in some bins in the $d\sigma_{jet}/d\eta$ and $d\sigma_{jet}/d\eta_{Lab}$ distributions. Hence, these bins are excluded from the analysis.

The NLOJET++ calculation is performed in the $\overline{\mathrm{MS}}$ scheme. The number of active flavours is set to five, the renormalisation scale is chosen to be E_{t}^2 of jets, and Q^2 is used as factorisation scale. The strong coupling $\alpha_s(\mu_r)$ is evolved at two loop precision and fixed at $\alpha_s(M_Z)$ to 0.118. The CTEQ5M1 parametrisation of the proton PDFs is used as input to NLOJET++. The theory uncertainty consists of the uncertainties due to the hadronisation correction and the renormalisation and factorisation scales. The latter are obtained by varying the two scales simultaneously by a factor of 4, i.e. $0.25 < \mu_{\mathrm{r}}^2/E_{\mathrm{t}}^2, \mu_{\mathrm{f}}^2/Q^2 < 4.0$. E_{t} as the renormalisation scale offers the benefit of smaller theory uncertainties compared to the Q scale.

6 Experimental Results and QCD Analysis

In the following, the results on the differential jet cross sections are presented, which are used to extract the strong coupling α_s.

6.1 Inclusive jet cross section

The measured inclusive jet cross sections are shown as function of $E_{\rm t}$ in four Q^2 bins, as function of Q^2 integrated over $E_{\rm t}$, and of $E_{\rm t}$ integrated over Q^2 in Figs. 4 - 6 and are compared to the NLO QCD calculations. In the lower part of Figs. 5 and 6, the ratio of the measured inclusive jet cross section to the NLOJET++ prediction is shown. The NLO calculation, corrected for hadronisation effects, gives a good description of the data in the full $E_{\rm t}$ and Q^2 range.

6.2 Determination of $\alpha_s(M_Z)$

We follow the methods in [1] and [6] to extract the strong coupling constant $\alpha_s(M_Z)$. The dependence of the cross section on $\alpha_s(M_Z)$ is determined in each Q^2-$E_{\rm t}$ (Fig. 4) and $E_{\rm t}$ (Fig. 6) bin by performing the NLOJET++ calculation using five values of $\alpha_s(M_Z)$ (0.110, 0.113, 0.116, 0.119 and 0.122). Using these five calculations per bin, the dependence of the cross section on $\alpha_s(M_Z)$ is then approximated by the function

$$\sigma_i(\alpha_s(M_Z)) = A_i \cdot \alpha_s(M_Z) + B_i \cdot \alpha_s^2(M_Z), \tag{1}$$

with the two free parameters determined in the fit. The function is then used to map the measured jet cross section $\alpha_s(M_Z)$ for each bin, as it is illustrated in Fig. 7 for one of the bins.

6.3 Results for $\alpha_s(M_Z)$ and $\alpha_s(E_t)$

The values of $\alpha_s(M_Z)$, determined from the inclusive jet cross sections measurements (Figs. 4, 6) in the Q^2-$E_{\rm t}$ and $E_{\rm t}$ bins, are shown in Fig. 8 and Fig. 9, respectively. The results on $\alpha_s(M_Z)$ are subsequently evolved using the two loop solution of the renormalisation group equation to $\alpha_s(E_{\rm t})$, where $E_{\rm t}$ corresponds to the mean value of $E_{\rm t}$ in the bin considered. The results are in good agreement with the world average $\alpha_s(M_Z) = 0.1187 \pm 0.0020$ [8].

6.4 Averaged $\alpha_s(M_Z)$

As the determinations of $\alpha_s(M_Z)$ are consistent over the whole Q^2 and E_t range, they can be combined into one average value. Due to correlations of the measured cross sections, the individual values of $\alpha_s(M_Z)$ are also correlated. We use the method presented in [1] and [7] to obtain a combined fit to the 15 $\alpha_s(M_Z)$ determinations in four Q^2 bins (Fig. 8). This procedure gives $\chi^2/\mathrm{ndf} = 20.14/14 = 1.44$, and the average $\alpha_s(M_Z)$ value is

$$\alpha_s(M_Z) = 0.1197 \ \pm 0.0016\,(\mathrm{exp.})\,{}^{+0.0046}_{-0.0048}\,(\mathrm{th.}). \tag{2}$$

The largest contribution to the experimental error is due to the LAr energy scale and the model dependence. The renormalisation and factorisation scale variations are the major contribution to the theory uncertainty.

The averaged $\alpha_s(M_Z)$ and corresponding $\alpha_s(E_t)$ values are shown in Fig. 9. The averaged $\alpha_s(M_Z)$ value is consistent with the world average and with the previous H1 inclusive jet result [1] : $\alpha_s(M_Z) = 0.1186\ \pm 0.0030\,(\mathrm{exp.})\,^{+0.0039}_{-0.0045}\,(\mathrm{th.})$.

7 Summary

Measurements of inclusive jet cross sections in deep inelastic positron-proton scattering in the range of $150 < Q^2 < 5000\,\mathrm{GeV}^2$ and transverse jet energy $E_\mathrm{t} > 7$ GeV have been presented. Predictions obtained with the NLO QCD program NLOJET++ provide a good description of the single and double differential inclusive jet cross sections. A determination of $\alpha_s(M_Z)$ yields

$$\alpha_s(M_Z) = 0.1197\ \pm 0.0016\,(\mathrm{exp.})\,^{+0.0046}_{-0.0048}\,(\mathrm{th.}). \tag{3}$$

This value is consistent with the world average of $\alpha_s(M_Z)$.

References

[1] H1 Collaboration, C. Adloff *et al.*, Eur. Phys. J. C19 (2001) 289;
Markus Wobisch, Ph. D thesis, PITHA 00/12.

[2] B. R. Webber, J. Phys. **G19** (1993) 1567.

[3] H1 Collaboration, I. Abt *et al.*, Nucl. Instr. Meth. A386 (1997) 310 and 348.

[4] M. H. Seymour, KTCLUS program.

[5] Z. Nagy and Z. Trocsanyi, Phys. Rev. Lett. 87 (2001) 082001.

[6] ZEUS Collaboration, S. Chekanov *et al.*, Phys. Lett. B547 (2002) 164;
H. Raach, Ph. D thesis, DESY-THESIS-2001-046.

[7] G. Lobo, C. Pascaud and F. Zomer, H1-01/98-536.

[8] S. Eidelman *et al.* [Particle Data Group Collaboration], Phys. Lett. B **592** (2004) 1.

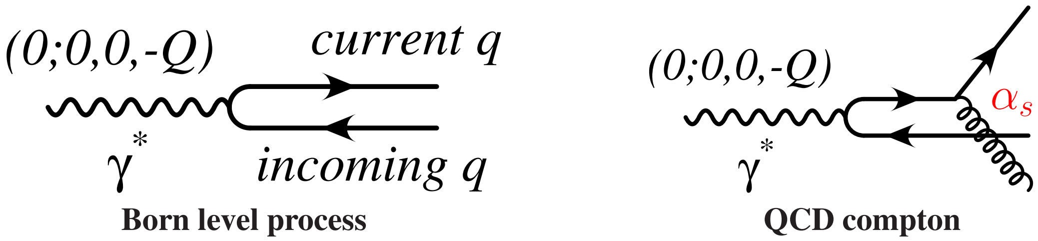

Figure 1: Deep inelastic scattering in the Breit frame, (a) Born level process and (b) QCD Compton process.

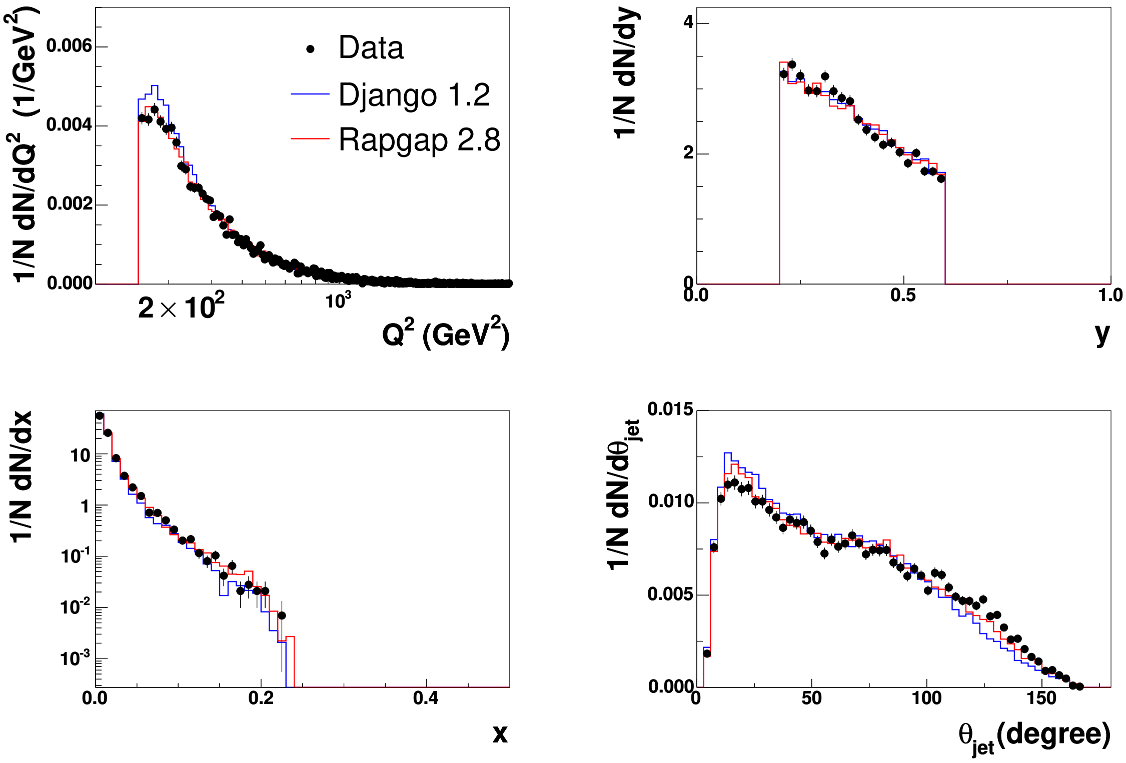

Figure 2: Kinematic variables and jet polar angle of the DIS inclusive jet sample, the distributions are normalised to one and are compared to MC model predictions.

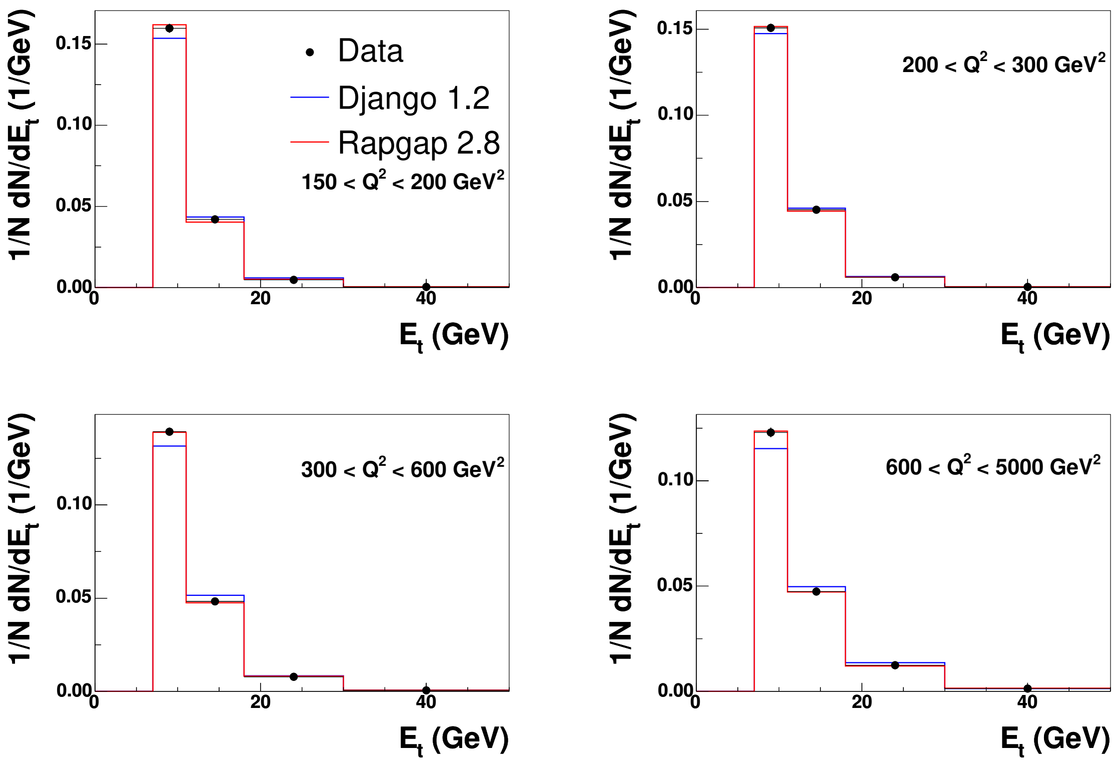

Figure 3: Jet transverse energy E_t in four Q^2 bins, the distributions are normalised to one and are compared to MC model predictions.

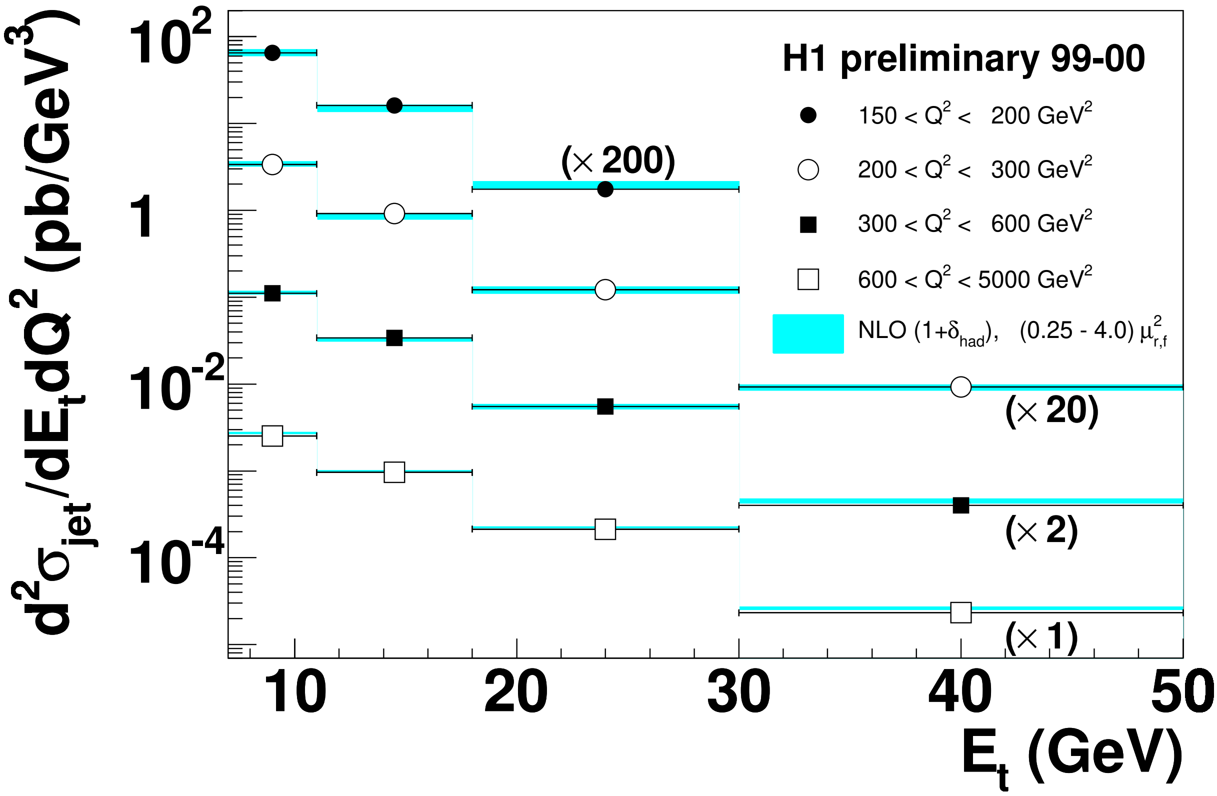

Figure 4: Measured $d\sigma/dE_t$ in four Q^2 bins compared with NLOJET++ predictions corrected for hadronisation effects. The bands show the theoretical uncertainty by varying the renormalisation and factorisation scales by a factor of two.

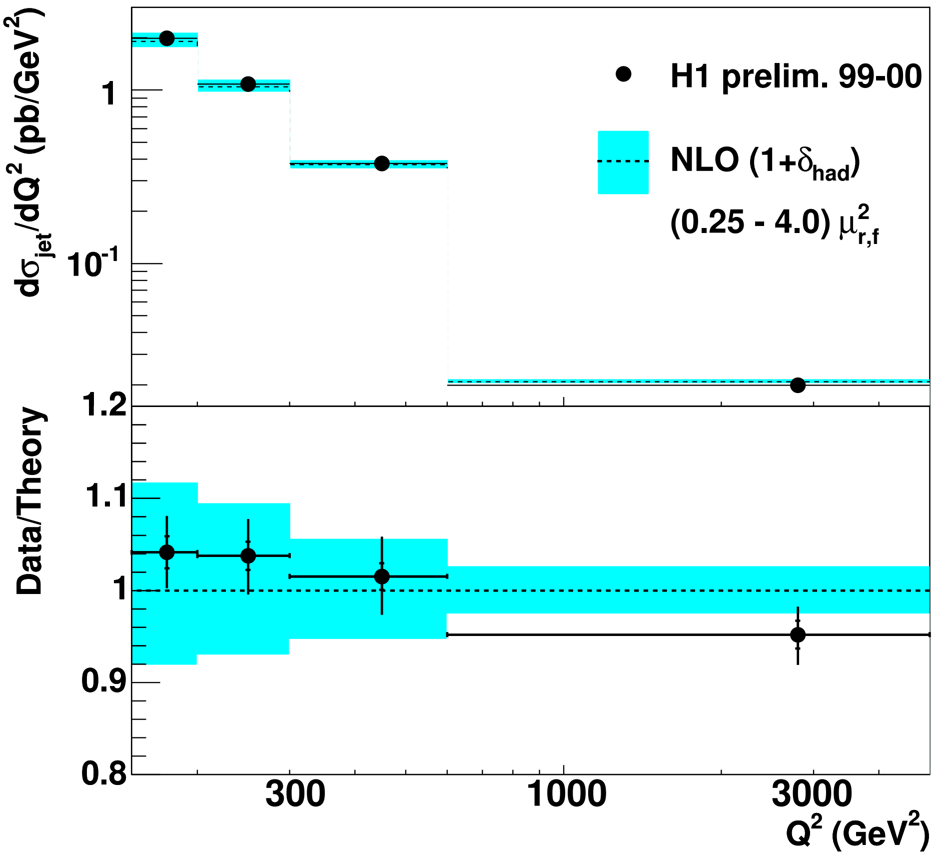

Figure 5: Measured $d\sigma/dQ^2$ (integrated over the transverse jet energy E_t) compared with NLO-JET++ predictions corrected for hadronisation effects. The band shows the theory uncertainty by varying the renormalisation and factorisation scales by a factor of two. The statistical uncertainty is shown as the inner error bar, while the total error is denoted by the outer error bar.

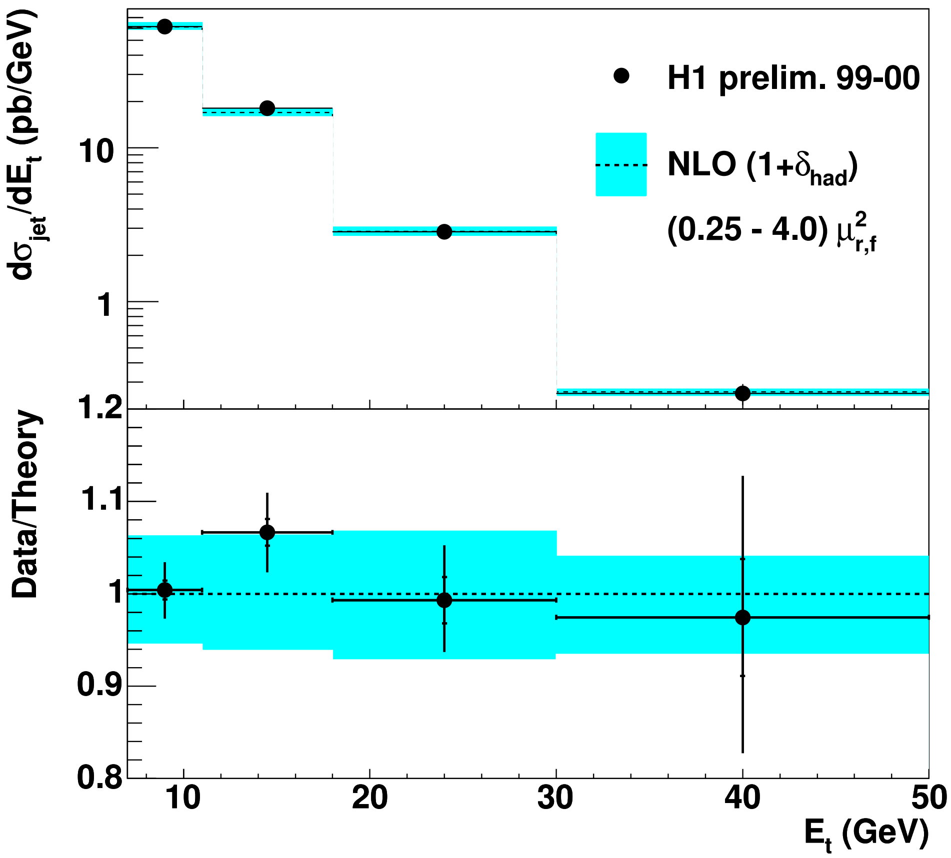

Figure 6: Measured $d\sigma/dE_\mathrm{t}$ (integrated over Q^2) compared with NLOJET++ predictions corrected for hadronisation effects. The bands show the theory uncertainty by varying the renormalisation and factorisation scales by a factor of two. The statistical uncertainty is shown as the inner error bar, while the total error is denoted by the outer error bar.

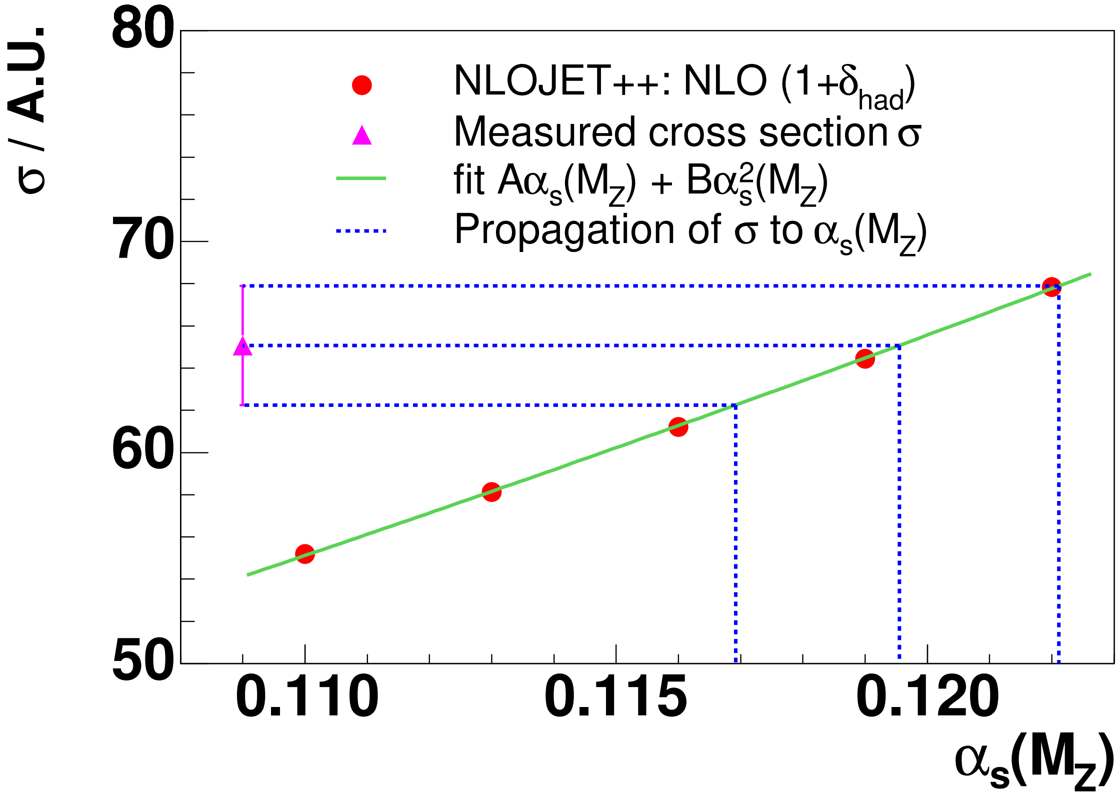

Figure 7: Extraction of the strong coupling constant $\alpha_s(M_Z)$ from the measured inclusive jet cross section for a given bin in Q^2 and E_{t}. The cross section is given in arbitrary units.

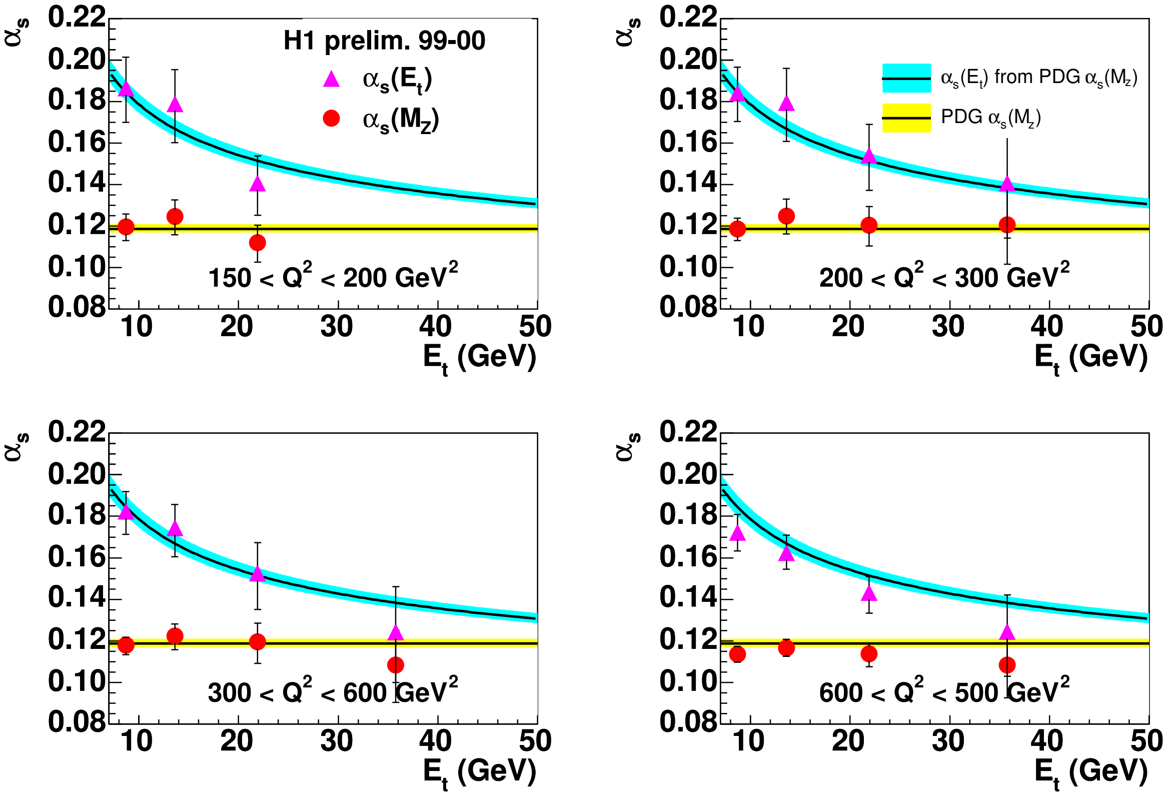

Figure 8: Results for $\alpha_s(M_Z)$ and $\alpha_s(E_t)$, where the $\alpha_s(E_t)$ values have been evolved from the measured $\alpha_s(M_Z)$ values using the two loop solution of the renormalisation group equation. The curves with error bands show values corresponding to the world average $\alpha_s(M_Z) = 0.1187 \pm 0.0020$.

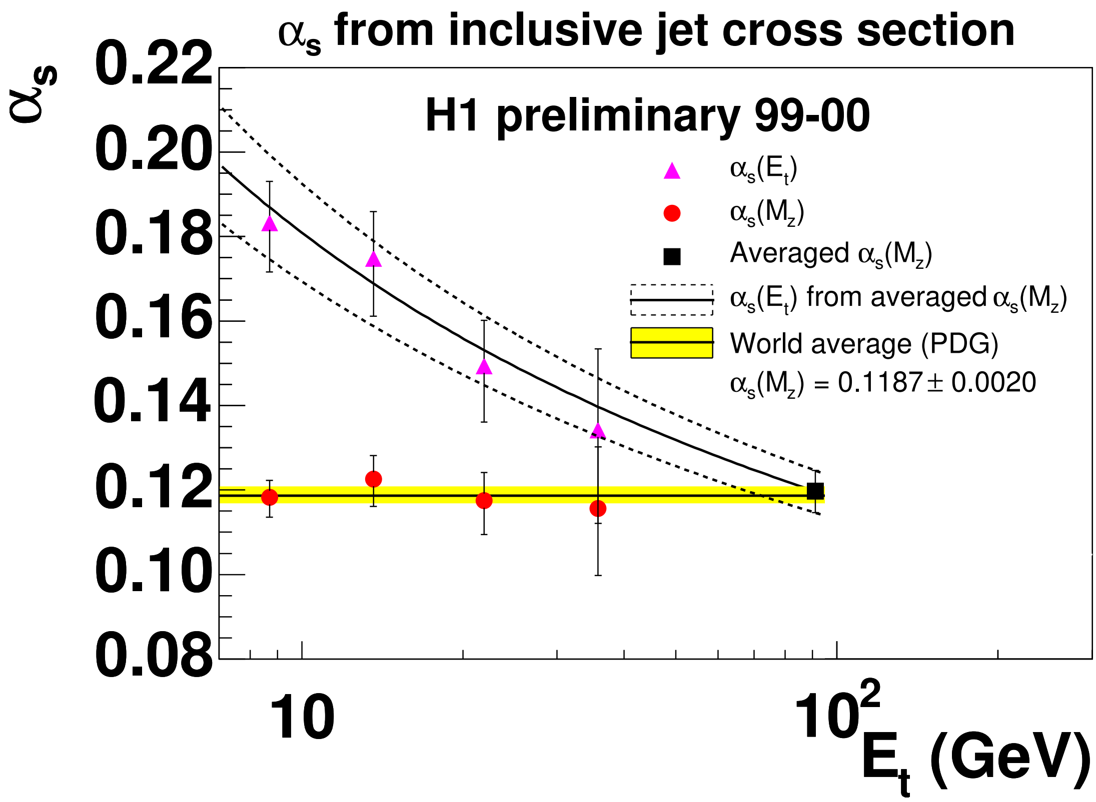

Figure 9: Results for $\alpha_s(M_Z)$ and $\alpha_s(E_t)$, where the $\alpha_s(E_t)$ values have been evolved from the measured $\alpha_s(M_Z)$ values for each bin in $E_{\rm t}$ (integrated over Q^2) using the two loop solution of the renormalisation group equation. The solid curve shows the result of evolving the averaged (over the 15 Q^2 - $E_{\rm t}$ bins) $\alpha_s(M_Z)$, while the dashed curves indicate the respective error band. The horizontal line with the shaded error band corresponds to the world average $\alpha_s(M_Z) = 0.1187 \pm 0.0020$.